International Journal of Astrobiology 13 (4): 353–365 (2014)
doi:10.1017/S1473550414000366 © Cambridge University Press 2014

Spectral features of biogenic calcium carbonates and implications for astrobiology

B. L. Berg[1], J. Ronholm[2], D. M. Applin[1], P. Mann[1], M. Izawa[1], E. A. Cloutis[1] and L. G. Whyte[2]

[1]*Department of Geography, University of Winnipeg, Winnipeg, Manitoba, Canada*
e-mail: e.cloutis@uwinnipeg.ca
[2]*Department of Natural Resource Sciences, McGill University, Sainte-Anne-de-Bellevue, Quebec, Canada*

Abstract: The ability to discriminate biogenic from abiogenic calcium carbonate ($CaCO_3$) would be useful in the search for extant or extinct life, since $CaCO_3$ can be produced by both biotic and abiotic processes on Earth. Bioprecipitated $CaCO_3$ material was produced during the growth of heterotrophic microbial isolates on medium enriched with calcium acetate or calcium citrate. These biologically produced $CaCO_3$, along with natural and synthetic non-biologically produced $CaCO_3$ samples, were analysed by reflectance spectroscopy (0.35–2.5 μm), Raman spectroscopy (532 and 785 nm), and laser-induced fluorescence spectroscopy (365 and 405 nm excitation). Optimal instruments for the discrimination of biogenic from abiogenic $CaCO_3$ were determined to be reflectance spectroscopy, and laser-induced fluorescence spectroscopy. Multiple absorption features in the visible light region occurred in reflectance spectra for most biogenic $CaCO_3$ samples, which are likely due to organic pigments. Multiple fluorescence peaks occurred in emission spectra (405 nm excitation) of biogenic $CaCO_3$ samples, which also are best attributed to the presence of organic compounds; however, further analyses must be performed in order to better determine the cause of these features to establish criteria for confirming the origin of a given $CaCO_3$ sample. Raman spectroscopy was not useful for discrimination since any potential Raman peaks in spectra of biogenic carbonates collected by both the 532 and 785 nm lasers were overwhelmed by fluorescence. However, this also suggests that biogenic carbonates may be identified by the presence of this organic-associated fluorescence. No reliable spectroscopic differences in terms of parameters such as positions or widths of carbonate-associated absorption bands were found between the biogenic and abiogenic carbonate samples. These results indicate that the presence or absence of organic matter intimately associated with carbonate minerals is the only potentially useful spectral discriminator for the techniques that were examined, and that multiple spectroscopic techniques are capable of detecting the presence of associated organic materials. However, the presence or absence of intimately associated organic matter is not, in itself, an indicator of biogenicity.

Received 1 July 2014, accepted 7 August 2014

Key words: biomarkers, biomineralization, carbonates, exobiology, Mars, spectroscopy.

Introduction

Current and upcoming Mars exploration missions are targeted towards habitability, and the detection of extant or extinct life through *in situ* exploration and future sample return missions. Currently, Mars is a cold desert considered to be inhospitable to life; it is postulated that if life were to exist on Mars, its presence could be detected through biomarkers indicating past life or biological activity (Banfield *et al.* 2001). There has been evidence for the presence of liquid water on the surface and subsurface of early Mars, which would have been conducive to the development and support of life (McKay 1997). It has been hypothesized that geological and environmental conditions of Early Mars were similar to those of Early Earth, in which conditions were warm and wet (Davis & McKay *et al.* 1996; McKay 1997; Cockell *et al.* 2000; Holm & Andersson 2005; Edwards 2010). It has been suggested that if life originated on Mars during this time, it may have been similar to microorganisms living in extreme environments on Earth today (McKay 1997; Raulin & McKay 2002; Simoneit 2004; Delaye & Lazcano 2005; Edwards 2010).

Recently, carbonates have been detected at several sites on Mars, such as in the Nili Fossae region (Ehlmann *et al.* 2008), in the Columbia Hills of Gusev crater (Morris *et al.* 2010) and in Leighton crater (Michalski & Niles 2010). Carbonates have also been detected in Martian meteorite ALH84001, and have been thought to be of biological origin (McKay *et al.* 1996), however not without dispute (e.g. Vecht & Ireland 2000). Of particular interest to our study, calcium carbonate has tentatively been detected in soils at the Phoenix Landing Site (Boynton *et al.* 2009).

On Earth, calcium carbonate ($CaCO_3$) can be formed by biomineralization, diagenetic processes, or abiotic processes (Tucker & Wright 1990; Stalport *et al.* 2005). $CaCO_3$ is one of the most commonly produced biominerals, and it can be produced under strict genetic control (biologically controlled

https://doi.org/10.1017/S1473550414000366 Published online by Cambridge University Press

mineralization), as seen in eukaryotes, or in the form of a by-product (biologically induced mineralization), as seen in prokaryotes (Mann 2001). Six $CaCO_3$ polymorphs exist, in which calcite and aragonite are the most stable and most commonly formed by biomineralization (Mann 2001; Ehrlich 2002).

There are numerous minerals that can be produced by both biogenic and abiogenic processes on Earth, which highlights the need for determining a method to differentiate between them. Factors that may indicate biogenicity of a mineral include, but are not limited to: specific phases, major element composition, trace elements, isotopic composition, crystal morphology, surface composition and morphology, spatial arrangement, and the presence of organic molecules indicating biomineralization (Banfield *et al.* 2001). In order to determine the biogenicity of a sample from Mars, it would first be necessary to establish reliable criteria that differentiate minerals that are biologically produced from their non-biologically produced counterparts. Similarly, the determination of an optimal instrument able to detect these differences and to be included on future missions involving rovers or landers would be extremely useful in the detection of biomarkers in planetary exploration.

Some work has been done on characterizing differences between biogenic and abiogenic $CaCO_3$, however much of the work has focused on differential thermal analysis (Stalport *et al.* 2005, 2008), and analysis of thermally processed carbonates using infrared spectroscopy (Orofino *et al.* 2007, 2009; Blanco *et al.* 2013). Our study aims to establish discrimination criteria using samples that have not been thermally altered in order to provide a baseline for future studies. Instead, spectroscopic techniques were used since they allow for the non-destructive analysis of samples without sample preparation, facilitating *in situ* analyses. The instruments that were applied to the analysis of biogenic and abiogenic samples include some that are available on orbiting platforms, such as reflectance spectrometers (Bibring *et al.* 2005; Murchie *et al.* 2007), and others that have been proposed for future landers/rovers, including reflectance spectroscopy, Raman and laser-induced fluorescence (Storrie-Lombardi & Sattler 2009; Pilorget *et al.* 2012; Korablev *et al.* 2013; De Angelis *et al.* 2014). A companion study is evaluating how and if any spectral differences are altered after exposure to simulated Martian conditions.

In order to investigate potential criteria and optimal instruments for the discrimination of biogenic from abiogenic $CaCO_3$, we analysed bioprecipitated material collected from microbial isolates taken from Mars analogue sites within the Canadian High Arctic (Steven *et al.* 2007) and Antarctica (Goordial personal communication). In this study, biologically produced and non-biologically produced $CaCO_3$ were analysed by reflectance spectroscopy, Raman spectroscopy, and laser-induced fluorescence spectroscopy. The spectral differences between biogenic and abiogenic carbonates will be useful in evaluating how these minerals could be distinguished by a planetary rover or lander in the search for extant or extinct life.

Materials and methods

Biological precipitation of calcium carbonates

Each biogenic $CaCO_3$ sample was precipitated during the growth of several heterotrophic bacteria isolated from Polar soil and endolith samples, as outlined in Ronholm *et al.* (in press). A culture collection ($\sim$ 300 isolates) was screened for the ability to precipitate $CaCO_3$ crystals. B4 Media (Boquet *et al.* 1973) (4 g of yeast extract, 10 g glucose, 15 g bacteriological agar and either 2.5 g calcium acetate or 2.5 g calcium citrate per litre of media) was streaked with each isolates and grown for 4 weeks in a humidity controlled environmental chamber at 22 °C. After 4 weeks each isolate was inspected for visual signs of $CaCO_{3(s)}$ precipitation on both calcium acetate and calcium citrate supplemented media. Several, but not all, isolates produced macroscopic crystals on one or both media types (Table 1). Negative control B4 plates were incubated under the same conditions without being inoculated with bacterial cultures; crystals did not form on these plates.

Biogenic $CaCO_3$ was separated from growth media and bacteria by scraping the mineral/bacteria mixture off the surface of solid media using a sterile inoculation loop. Biogenic $CaCO_3$ was separated from the bacteria by successive rounds of sedimentation in millipure water (Sánchez-Román *et al.* 2011) Precipitates were then dried on the low setting using a rotary evaporator and stored at room temperature until examination. The abiogenic carbonates included for comparison were naturally occurring (likely hydrothermal) monocrystalline or coarsely-crystalline aggregates of aragonite (CRB120 and CRB125), calcite (CRB131) and a synthetic calcite (PIG004). Descriptions of these samples and the biogenic samples are provided in Table 2.

X-ray diffractometry

The identities of the biogenic and abiogenic samples included in this study were confirmed by X-ray diffractometry (XRD), and shown in Tables 1 and 2. XRD analysis was carried out using a Bruker D8 Discover diffractometer at the University of Winnipeg using Co $K\alpha_{1,2}$ radiation ($\lambda = 1.78897$ Å), accelerating voltage 40 kV and 40 mA beam current. X-ray diffraction patterns were collected with a step size 0.02° and counting time of 10 s per step covering 10–70°2θ.

Reflectance spectroscopy

Reflectance spectra over the 0.35–2.5 μm range were acquired with an Analytical Spectral Devices (ASD) FieldSpec Pro high-resolution (HR)® spectrophotometer. The spectral resolution of the instrument varies between 2 and 7 nm and spectral sampling is done at 1.4 nm intervals. The instrument internally resamples the data to 1 nm intervals with a third-order polynomial. Spectra were acquired at $i = 30°$ and $e = 0°$ using the FieldSpec Pro. Illumination was provided by an in-house 100 W quartz-tungsten-halogen (QTH) bulb directed into a fibre assembly through an aluminium light pipe. A total of 500 spectra were averaged to improve the signal-to-noise ratio (SNR). Reflectance spectra were measured relative to a calibrated Spectralon® disk. Wavelength calibration was

https://doi.org/10.1017/S1473550414000366 Published online by Cambridge University Press

Table 1. *Sample descriptions for biogenic calcium carbonate ($CaCO_3$) samples.*

Sample	Source of microbial isolate	Optimal substrate for $CaCO_3$ precipitation added to B4 media	$CaCO_{3(s)}$ polymorphs identified by μXRD	Major mineral morphologies identified (SEM)
Agromyces sp. ofe 5.5	Arctic soil	Calcium Acetate (CA)	Calcite	Euhedral
Arthrobacter sp. JG9	Antarctic endolith	Calcium Citrate (CC)	Calcite, Vaterite	Euhedral, Anhedral (Irregular, Spherulite, Globular,)
Arthrobacter sp. oc 825	Arctic Soil	CC	Calcite	Euhedral
Arthrobacter sp. ofe 4.2	Arctic Soil	CC	Calcite	Anhedral (Diskoid)
Arthrobacter sp. ofe 7.23	Arctic Soil	CC	Calcite	Anhedral (Flakey)
Arthrobacter sp. ofe 10.25	Arctic Soil	CC	Calcite, Aragonite	Euhedral, Anhedral (Globular, Hemi-spherulite, diskoid)
Arthrobacter sp. ofe 1.1	Arctic Soil	CA	Calcite	Euhedral
Arthrobacter sp. ofe 10.10	Arctic Soil	CA	Calcite	
Arthrobacter sp. ofe 3.1	Arctic Soil	CA	Calcite	Anhedral (Flakey)
Arthrobacter sp. ofe 8.9	Arctic Soil	CA	Calcite	Anhedral (Irregular, Flakey)
Arthrobacter sp. eur3 7.19	Arctic Soil	CA	Calcite	Anhedral (Flakey)
Arthrobacter sp. CY7	Arctic Soil	CC	Calcite	Euhedral, Anhedral (Flakey)
Ralstonia sp. ofe 1.3	Arctic Soil	CA	Calcite	Euhedral
Rhodococcus sp. JG12	Antarctic Endolith	CC	Calcite	Euhedral, Anhedral (Spherulite)
Rhodococcus sp. MD.2	Arctic Soil	CA	Calcite	
Rhodococcus sp. ofe 9.29	Arctic Soil	CC	Calcite	Anhedral (Spherulite)
Rhodococcus sp. CY5	Arctic Soil	CA	Calcite	Euhedral
Rhodococcus sp. CY6	Arctic Soil	CA	Calcite	
Rhodococcus sp. eur1 9.01.2	Arctic Soil	CA	Calcite	Euhedral
Rhodotorula mucilaginosa JG1 (yeast)	Antarctic Permafrost	CA	Calcite	Euhedral

monitored through regular measurements of a holmium oxide-doped Spectralon® standard. The spot size measured by this instrument is variable, depending on distance from probe to sample. For this study, a spot size of ~5 mm was used.

The ASD spectrometer has three detectors that collectively cover the full 0.35–2.5 μm range as follows: 0.35–1.0, 1.0–1.83 and 1.83–2.5 μm. As a result, there may be small discontinuities in the data where the detector changeovers occur (1.0 and 1.83 μm). These were removed by correcting the shortest (0.35–1.0 μm) and the longest (1.83–2.5 μm) intervals to the middle interval (1.0–1.83 μm), which is thermoelectrically cooled and temperature controlled.

Raman spectroscopy

Raman spectra were collected at the University of Winnipeg over the 175–4000 cm^{-1} range at a resolution of ~4 cm^{-1} at 614 nm with the B&WTek (Newark, DE) i-Raman-532-S instrument. Excitation was provided by a 532 nm ~50 mW BWN solid-state diode laser. Raman-scattered light was detected by a Glacier™ *T*, a high spectral resolution (0.08 nm) thermoelectrically cooled (14 °C) charge-coupled device (CCD) detector. The automatic integration time function (which increases integration time incrementally, until the response is close to saturation) was used, yielding an optimal SNR. Initial sample measurements were acquired with the BAC102 fibre optic attachment with a working distance of 5.9 mm that gives a theoretical spot size of 85 μm. The BAC102 fibre optic probe contains a long-pass OD6 notch filter, which filters reflected excitation light prior to interaction with the detector for an increased SNR. Samples were placed on an adjustable stage and were approached directly to the distance regulator prior to collection. Measurements for each sample were made by first acquiring a dark current spectrum, followed by measurement of the sample. Both measurements were made using an identical viewing geometry and integration time, and 10 averaged spectra. Raman-shift calibration was monitored through regular measurements of a polystyrene standard.

A DeltaNu Rockhound Raman spectrometer was used for complementary data collection in the 200–2000 cm^{-1} range with a thermoelectrically cooled (0 °C) CCD detector. A solid-state diode laser provided excitation of 100 mW at 785 nm. Theoretical spot size measured by the instrument is 25 μm. The instrument has a long pass OD6 notch filter. A spectral resolution of 7 cm^{-1}, an optimized integration time approaching signal detector saturation, and 10 averaged spectra were used to increase the SNR within each sample. The Rockhound instrument was mounted securely with the probe pointed 90° downwards. Samples were placed on an adjustable stage and were approached directly to the probe prior to collection. Prior to each sample collection, the instrument was calibration checked with a polystyrene standard.

Laser-induced fluorescence spectroscopy

Sample fluorescence was measured at the University of Winnipeg in the 200–1150 nm range with an Ocean Optics (Dunedin, Fl) Maya2000 PRO miniaturized spectrometer equipped with an HC-1 grating and 30 μm slit width, giving

https://doi.org/10.1017/S1473550414000366 Published online by Cambridge University Press

Table 2. *Sample descriptions for abiogenic calcium carbonate ($CaCO_3$) samples. All samples were crushed and dry sieved to a particle size of <45 μm.*

Sample	Source	$CaCO_{3(s)}$ polymorphs identified by μXRD
CRB120	Aragonite: from Silverton, Briscoe County, Texas, USA. Sample consists of iron oxyhydroxide-stained mm-sized crystal aggregates (from commercial supplier)	Aragonite
CRB125	Aragonite: Stiermark, Austria (from Smithsonian Institution National Museum of Natural History sample #B16198)	Aragonite
CRB131	Calcite: Axel Heiberg Island, NWT, Canada (collected by Michael Craig of the University of Western Ontario)	Calcite
PIG004	Synthetic (laboratory-produced calcite ($CaCO_3$): from Sigma Aldrich (ID: 23,921–6)	Calcite

us an effective spectral resolution between 0.48 nm at 200 nm and 0.46 nm at 400 nm. The detector is a 2D back-thinned linear CCD-array Hamamatsu S10420. Illumination was provided by one laser: a 75 mW 405 nm (Wicked Lasers, Tsim Sha Tsui, Kowloon, Hong Kong) and one spot light: UVP (Upland, CA) Black-Ray® B-100AP 100 W (21 700 uW cm^{-2} at a distance of two inches) spotlight with a 365 nm bandpass filter, that were independently directed through a bifurcated fibre optic bundle consisting of six illumination fibres surrounding a central pick-up fibre feeding into the detector array. This assembly consisted of 400 μm diameter solarization-resistant (XSR) fibres. A viewing geometry of $i = 0°$ and $e = 0°$ was used for all collections. An integration time of 150 ms with 500 averaged spectra were used to determine sample fluorescence at 365 nm. Fluorescence spectra were collected and interpreted in conjunction with the obtained Raman spectra, as discussed below.

Results and discussion

Our findings suggest that there are differences in spectral features between biogenic and abiogenic carbonates using a number of the applied spectroscopic techniques. There was no apparent correlation between medium type on which a given bacterial isolate was grown and $CaCO_3$-associated absorption band positions in reflectance, or emission bands in Raman or fluorescence spectra of their bioprecipitated material. Also, the genus of bacterial isolate responsible for $CaCO_3$ precipitation did not predict which spectral features are present. It should be cautioned that the attribution of a given peak to a given pigment or compound is not always definitive, and further analyses are planned to confirm the presence of specific compounds. The heterotrophic bacteria whose bioprecipitated material was analysed in this study are not known to carry out photosynthesis, therefore the spectral features observed cannot be attributed to photosynthetic pigments, such as chlorophylls, bacteriochlorophylls, or phycobilins.

Reflectance spectroscopy

All abiogenic and biogenic $CaCO_3$ samples showed an absorption feature at ~2.34 μm, which can be attributed to the second overtone of the asymmetric stretching mode ($3v_3$) of the carbonate ion (Table 3, Fig. 1(a)–(c)) (Gaffey 1987; Workman & Weyer 2012). Band depths for the 2.3 μm feature were similar for both biogenic and abiogenic carbonates. The band minimum wavelength for this feature varied slightly between samples, with the largest deviation seen between abiogenic aragonite (CRB120 and 125) and calcite (CRB131, PIG004), as expected (Gaffey 1987).

All biogenic samples and abiogenic aragonite sample CRB125 showed absorption features at both ~1.4 and ~1.9 μm, which were attributed to the presence of water within these samples (Fig. 1(a)–(c)) (Clark *et al.* 1990). It should be noted that this water is likely adsorbed, as pure $CaCO_3$ is anhydrous; therefore, these bands are not diagnostic of anhydrous carbonates.

Below 0.7 μm, biogenic carbonates showed a decrease in absolute reflectance and an increase in number of absorption features, except in *Rhodotorula mucilaginosa* (JG1), both features which were not seen in the abiogenic carbonates (e.g. Fig. 1(d)). Absorption features in the visible spectral range were attributed to the presence of pigmented compounds within the samples, possibly in trace amounts. All biogenic carbonates showed absorption features in the ~0.406–0.417 μm range. All biogenic carbonates except *R. mucilaginosa* (JG1), *Arthrobacter* sp. (oc825) and *Rhodococcus* sp. (eur3 9.01.3) showed absorption features in either or both of the ~0.444–0.459 μm and ~0.472–0.477 μm ranges. All biogenic carbonates except *R. mucilaginosa* (JG1) and *Arthrobacter* (ofe 10.10) had absorption features in either or both the 0.537–0.541 μm and 0.571–0.576 μm ranges. Some biogenic carbonates (*Ralstonia* sp. (ofe 1.3), *Arthrobacter* sp. (oc825), *Arthrobacter* sp. (cy7), *Arthrobacter* sp. (JG9), *Rhodococcus* (cy5), *Rhodococcus* sp. (eur3 9.01.3) and *Rhodococcus* sp. (JG12)) also showed absorption features in the ~0.498–0.503 μm region.

Absorption features within the range of 0.420–0.550 μm may be due to the presence of carotenoids, which are isoprenoid pigments that absorb strongly in the blue-green region (0.420–0.550 μm), which could lead to the appearance of yellow, orange or red coloration (Armstrong & Hearst 1996; Dworkin & Falkow 2006). The number of conjugated double bonds in the polyene chain of a given carotenoid plays an important role in the determination of its spectral properties (Armstrong & Hearst 1996). Although carotenoids are often associated with photosynthetic organisms, it has been shown that heterotrophic bacteria are capable of producing carotenoids for protection against environmental stress, such as cold temperatures and solar radiation (Dieser *et al.* 2010), as seen in the hostile environments from which isolates were sampled.

https://doi.org/10.1017/S1473550414000366 Published online by Cambridge University Press

https://doi.org/10.1017/S1473550414000366 Published online by Cambridge University Press

Table 3. *Band positions in reflectance spectra (2.3 μm, visible region, and near-infrared band minima), Raman spectra (v_1 symmetric stretch maxima and fluorescence peaks), and laser-induced fluorescence spectra for abiogenic and biogenic samples.*

Sample	Reflectance: 2.3 μm band minima	Reflectance: visible absorption band minima (μm)	Raman: v_1 symmetric stretch maxima (cm^{-1})	Raman: fluorescence peaks (nm)[a]	Laser-induced fluorescence: peak positions (nm)
CRB120 (aragonite)	2.32	None	1088	~ 594[b]	None
PIG004 (synthetic calcite)	2.34	None	1088	None[c]	None
CRB131 (calcite)	2.34	None	1088	~ 611[b]	None
CRB125 (aragonite)	2.32	None	1085	~ 596[b]	None
Arthrobacter sp. JG9	2.34	0.411[d], 0.459[e], 0.500[e], 0.538[e] and 0.574[e]	1085[f]	~ 596[b] and ~618[b]	576[e], 620[e] and 682[e]
Arthrobacter sp. oc825	2.34	0.411[d], 0.499[d], 0.539[d] and 0.574[d]	1085	~ 596[b] and ~618[b]	503[b], 620[d] and 682[d]
Arthrobacter sp. ofe 4.2	2.34	0.417[d], 0.446[d] 0.477[d], 0.539[e] and 0.573[d]	1092[f]	~ 596[b]	466[d] and 520[b,d]
Arthrobacter sp. ofe 7.23	2.34	0.413, 0.459[e], 0.537 and 0.573	1081[f]	~ 596[b] and 622	None
Arthrobacter sp. ofe 10.25	2.34	0.414, 0.451[d], 0.474, 0.541 and 0.576	1075[f]	~ 582 and ~630[b]	466[b,d], 520[b,d], 578[d], 620 and 682
Arthrobacter sp. ofe 1.1	2.34	0.410, 0.450[d], 0.475[d], 0.503[e],0.540 and 0.574	1082[f]	~ 586[b] and ~620	466[b], 498[b], 578, 620 and 682
Arthrobacter sp. ofe 10.10	2.34	0.415[e], 0.444[d] and 0.474[d]	1085	~ 596[b]	466[b,e], 520[b,e], 578[d], 620 and 682
Arthrobacter sp. ofe 3.1	2.34	0.411, 0.444, 0.476, 0.537 and 0.571	1085	~ 596[b] and ~618	466, 498[b], 580[d], 620 and 682[d]
Arthrobacter sp. ofe 8.9	2.34	0.410, 0.445, 0.477, 0.537 and 0.571	1075[f]	~ 596[b] and ~616[b]	466, 498[b], 580[d], 620 and 682[d]
Arthrobacter sp. eur3 7.19	2.34	0.410, 0.444, 0.476, 0.537 and 0.571	1085	~ 596[b] and ~618	466, 498[b], 580[d], 620 and 682[d]
Arthrobacter sp. cy7	2.34	0.410, 0.459[e], 0.501[e], 0.539 and 0.574	1085[f]	~ 596[b] and ~618	466[b,e] and 520[b,e]
Ralstonia sp. ofe 1.3	2.34	0.410, 0.477[e], 0.503[e], 0.540[d] and 0.574[d]	1085	~ 596[b]	503[b], 620[d] and 682[d]
Rhodococcus sp. JG12	2.34	0.411[d], 0.459[e], 0.500[e], 0.538[d] and 0.574[d]	1085[f]	~ 585[b], ~596[b] and ~618[b]	466[b], 520[b], 578, 620 and 682
Rhodococcus sp. ofe 9.29	2.34	0.412, 0.447, 0.472, 0.538 and 0.574	1075[f]	~ 608[b,g]	466[d], 498[b,d], 580 and 682[d]
Rhodococcus sp. cy5	2.34	0.411[e], 0.459[e], 0.500[e], 0.538[d] and 0.574[d]	1085	~ 596[b]	503[b], 620[d] and 682[d]
Rhodococcus sp. eur3 9.01.3	2.34	0.406[d], 0.498[e], 0.538[e] and 0.572[e]	1085	~ 596[b]	503[b], 620[d] and 682[d]
Rhodotorula mucilaginosa JG1 (yeast)	2.34	None	1088	~ 596[b]	503[b], 620 and 682

[a] Raman spectra plotted in wavelength rather than inverse centimetres.
[b] Maximum of a broad band.
[c] Minor/irrelevant fluorescence.
[d] Weak.
[e] Very weak.
[f] Inadequate signal above fluorescence to assign a reliable position.
[g] No clear maximum.
Note: 2.3 μm region absorption bands are reported to the nearest 10 nm. Visible region absorption bands are reported to the nearest 1 nm.

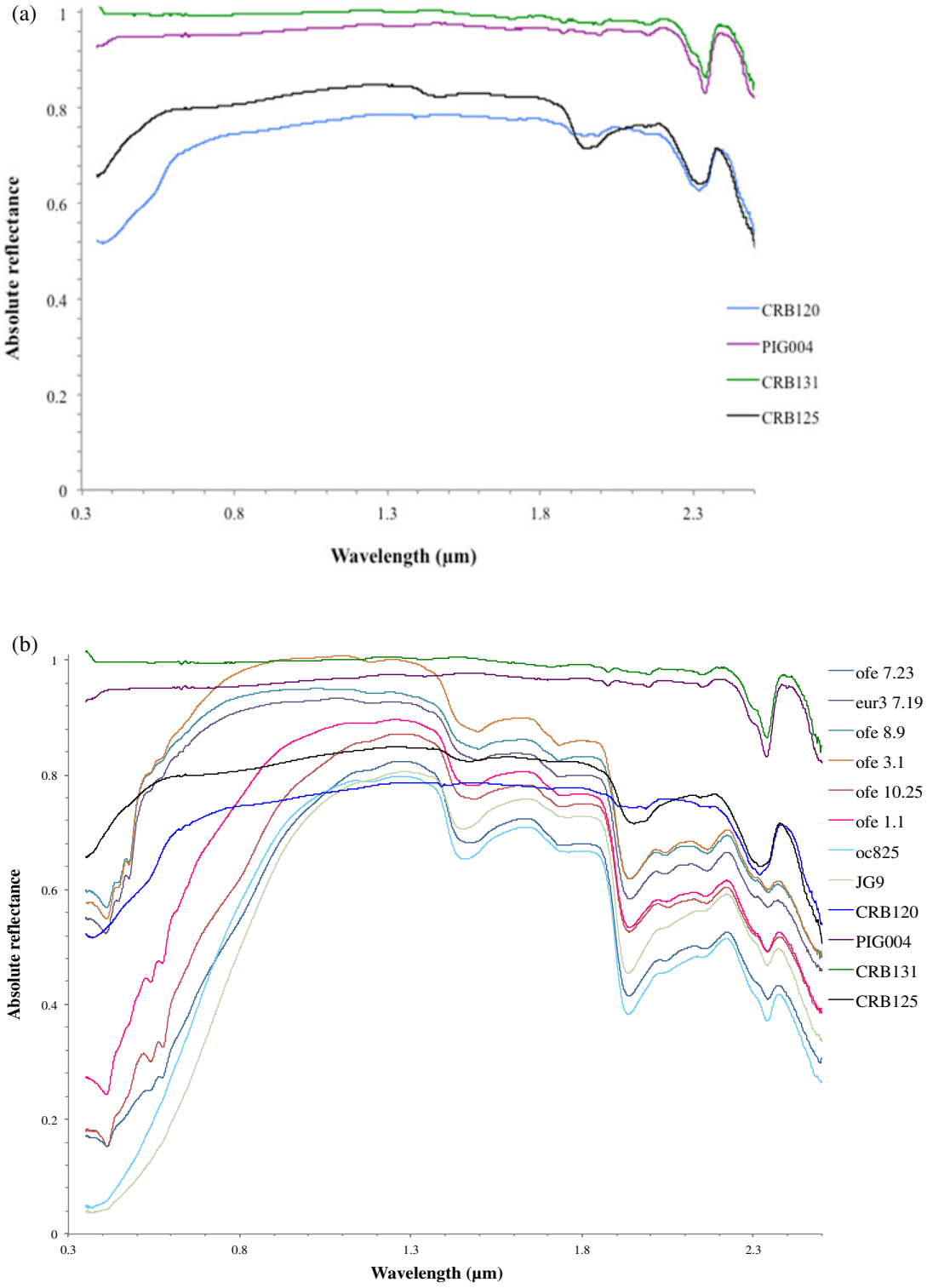

Fig. 1. For legend see next page.

However, the reflectance spectrum for minerals formed by *R. mucilaginosa* (JG1), a strain of yeast that normally produces carotenoids and appears pink during growth (Moore *et al.* 1989), did not show absorption features in the visible region. One possible explanation for this exception is that the concentration of carotenoids was too low to result in measurable absorption features.

Absorption features between 0.400 and 0.630 μm may have also been due to the presence of cytochromes, which are pigments containing an iron-containing porphyrin (haem) prosthetic group involved in cellular respiration and electron transfer (Thöny-Meyer 1997). In reduced cytochromes, there are three strong absorption features in the ultraviolet to visible spectrum called the α, β and γ, or Soret, peaks

https://doi.org/10.1017/S1473550414000366 Published online by Cambridge University Press

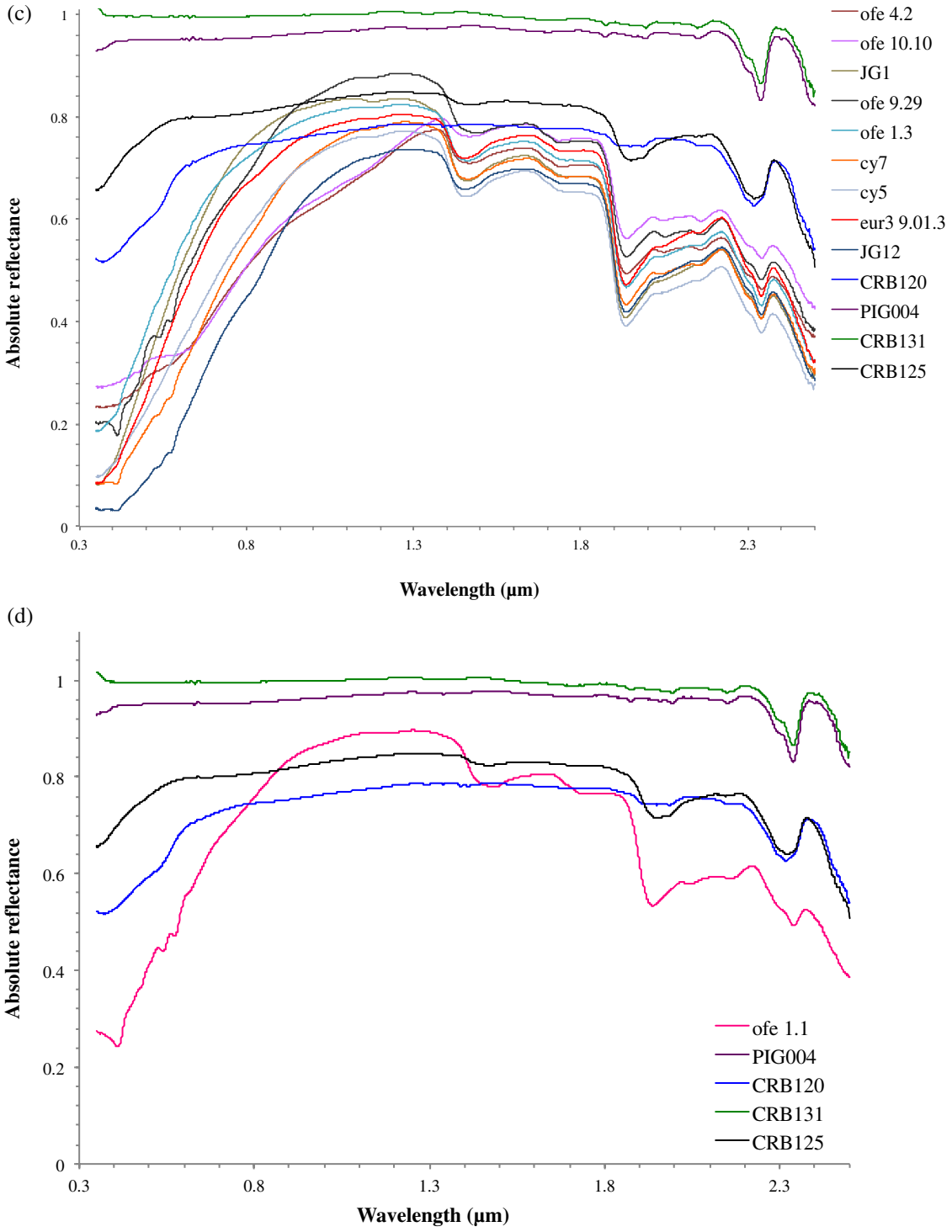

Fig. 1. (a) Reflectance spectra (0.35–2.5 μm) of abiogenic aragonite (CRB120 and CRB125) and calcite (CRB131 and PIG004). (b) Reflectance spectra (0.35–2.5 μm) of abiogenic aragonite (CRB120 and CRB125), abiogenic calcite (CRB131 and PIG004) and various biogenic $CaCO_3$ samples: ofe 7.23, eur3 7.19, ofe 8.9, ofe 3.1, ofe 10.25, ofe 1.1, oc825 and JG9. Absorption bands in the 1.4 and 1.9 μm regions are likely due to adsorbed water and are not diagnostic of anhydrous carbonates. Characteristic carbonate absorption features are present near 2.3 microns. Absorption bands attributable to organic compounds are present in the visible spectral region (narrow absorption bands below ~0.7 μm, as well as in the 1.7 and 2.0–2.2 μm regions, due to various organic (C–H) molecules (e.g. Izawa *et al.* 2014). (c) Reflectance spectra (0.35–2.5 μm) of abiogenic aragonite (CRB120 and CRB125), abiogenic calcite (CRB131 and PIG004) and various biogenic $CaCO_3$ samples: ofe 4.2, ofe 10.10, JG1, ofe 9.29, ofe 1.3, cy7, cy5, eur3 9.01.3 and JG12. (d) Reflectance spectra (0.35–2.5 μm) of abiogenic aragonite (CRB120 and CRB125), abiogenic calcite (CRB131 and PIG004) and biogenic $CaCO_3$ (represented by sample ofe 1.1). Multiple absorption features in the visible light region, and a decrease in absolute reflectance are present for biogenic $CaCO_3$, but are absent in abiogenic samples.

https://doi.org/10.1017/S1473550414000366 Published online by Cambridge University Press

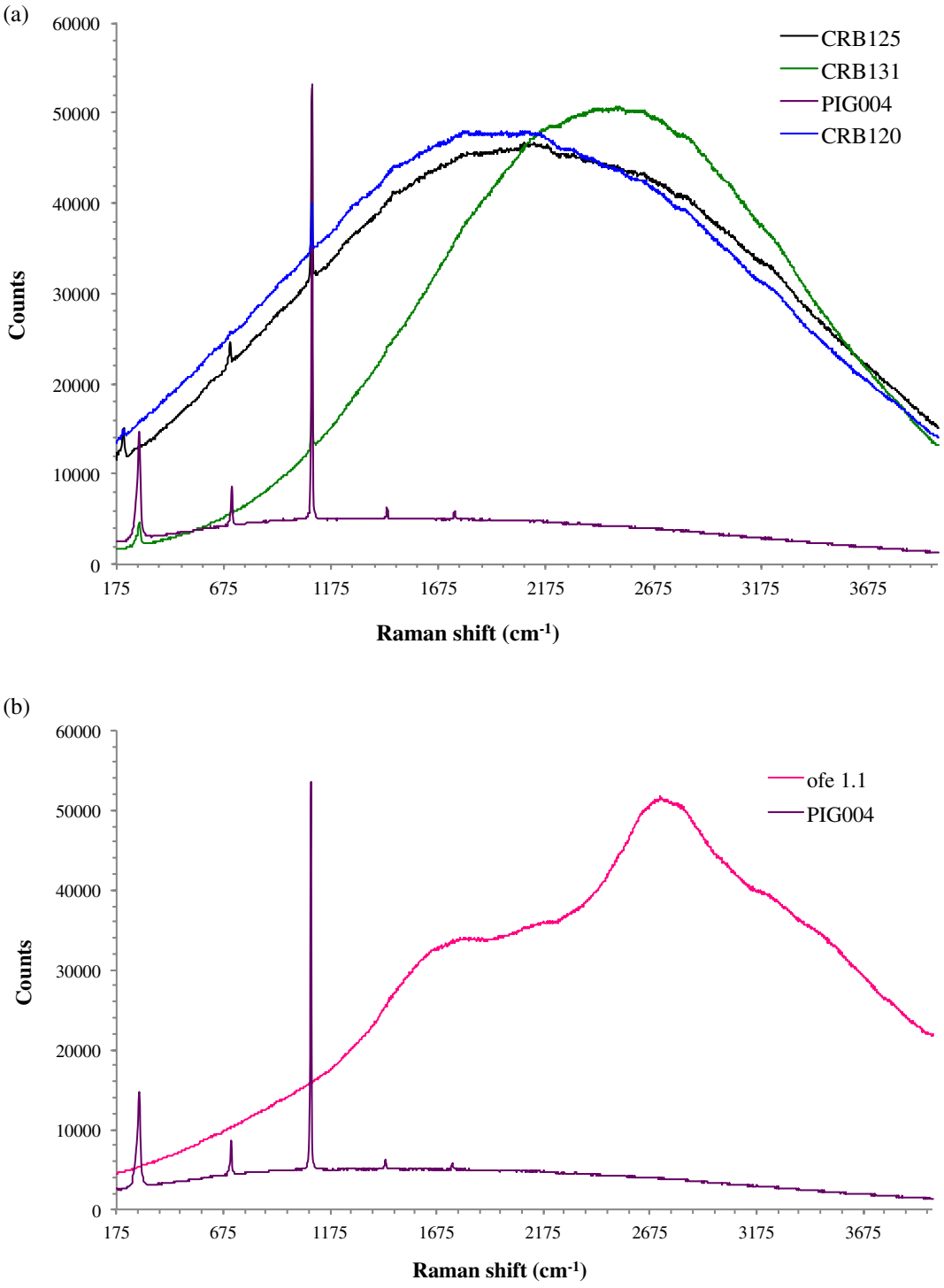

Fig. 2. For legend see next page.

(Thöny-Meyer 1997). Different spectral features exist for different types of cytochromes, in which the α peak (0.550–0.630 μm) can be used to classify the type of cytochrome present in a sample (Thöny-Meyer 1997). Oxidized cytochromes absorb in the 0.390–0.420 μm range (Soret region), and may also be related to the observed absorption features in the studied biogenic carbonates (Barton 2005).

An alternative explanation for the absorption of light in the visible and near-infrared region could be due to colour centres within the lattice structure of the bioprecipitated carbonates. Colour centres are caused by an unpaired electron, in which there can be an extra electron at a vacancy, a missing electron where there is usually a pair of electrons, or an unpaired electron can move to an excited state upon light absorption (Schulman & Compton 1962; Nassau 1978). Crystal lattices of

https://doi.org/10.1017/S1473550414000366 Published online by Cambridge University Press

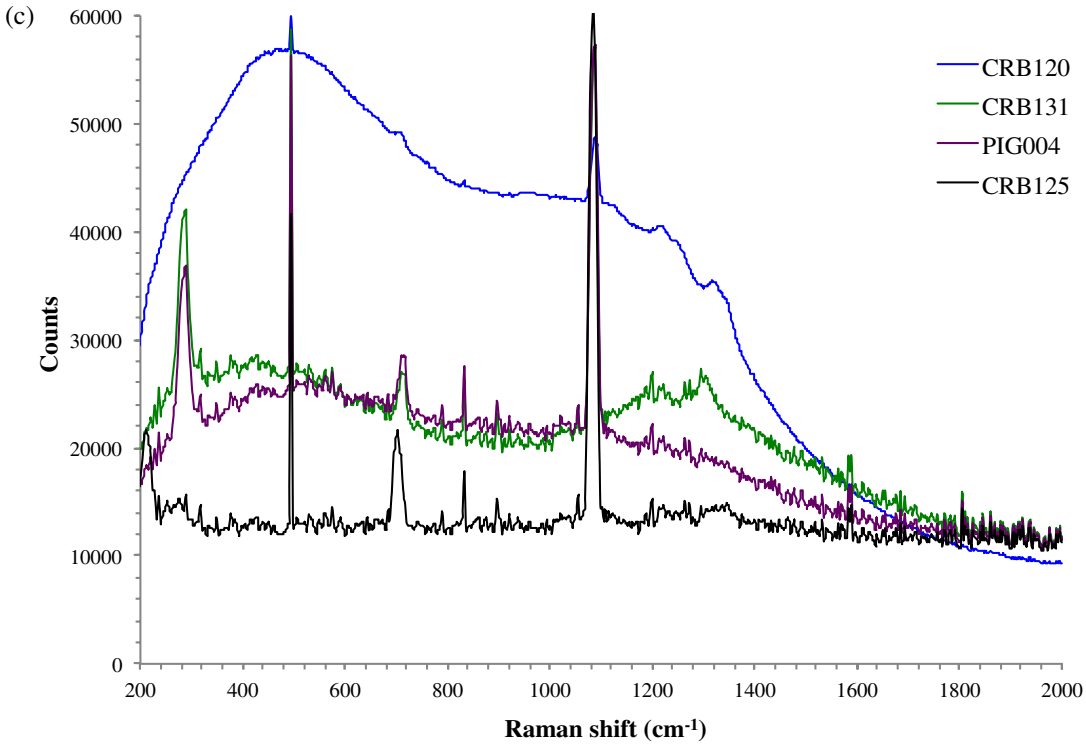

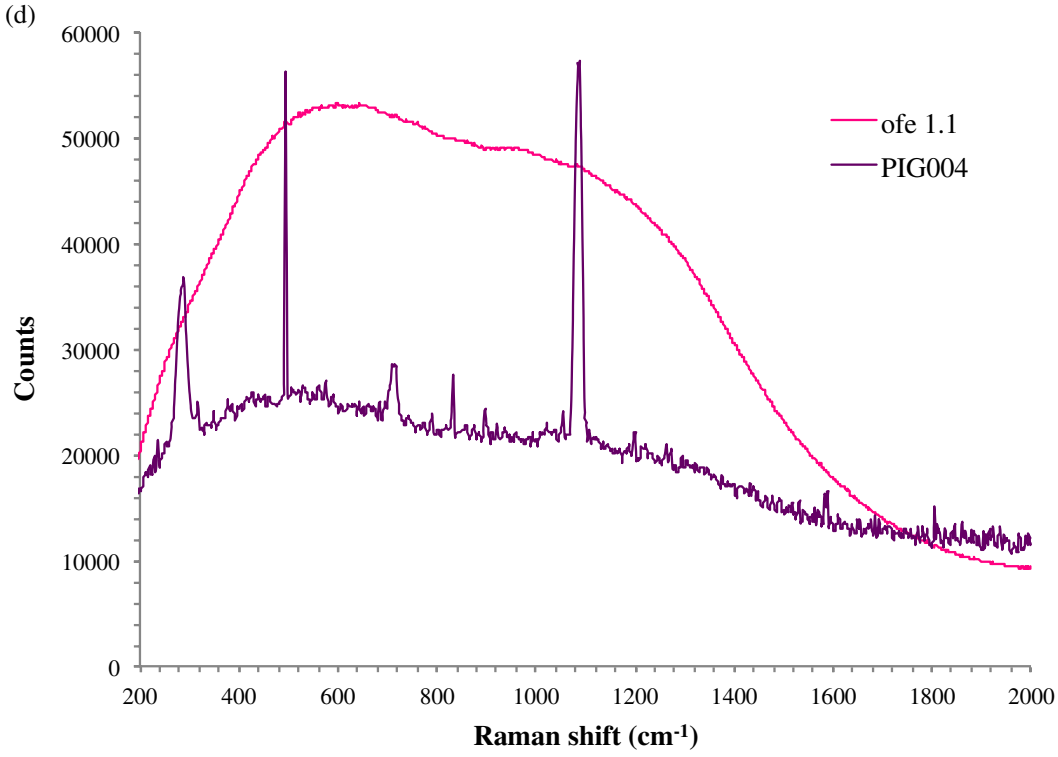

Fig. 2. (a) Raman spectra (175–4000 cm^{-1}) of abiogenic aragonite (CRB120 and CRB125) and calcite (PIG004 and CRB131) collected with a 532 nm laser. (b) Raman spectra (175–4000 cm^{-1}) of abiogenic calcite (PIG004) and biogenic $CaCO_3$ (represented by sample ofe 1.1) collected with a 532 nm laser. (c) Raman spectra (175–4000 cm^{-1}) of abiogenic aragonite (CRB120 and CRB125) and calcite (PIG004 and CRB131) collected with a 785 nm laser. (d) Raman spectra (175–4000 cm^{-1}) of abiogenic calcite (PIG004) and biogenic $CaCO_3$ (represented by sample F4B3) collected with a 785 nm laser.

https://doi.org/10.1017/S1473550414000366 Published online by Cambridge University Press

minerals have defects that occur naturally, and include vacancies, interstitials, and substituted impurities (Schulman & Compton 1962). However, colour centres usually result in broad and weak absorption features (Nassau 1978).

The presence of various organic molecules is also evident from absorption features seen in the biogenic sample spectra in the 1.7 and 2.0–2.2 μm regions in particular. These are generally attributable to various organic molecules, specifically C–H overtone and combination bands, although other compounds such as N-bearing molecules may also contribute to absorptions in these regions (e.g. Izawa *et al.* 2014).

Raman spectroscopy

Raman spectra of abiogenic $CaCO_3$ samples with the 532 nm laser showed the presence of Raman peaks, whereas any potentially present Raman peaks were overwhelmed by sample fluorescence in spectra for biogenic carbonates (Table 3, Fig. 2(a) and (b)). Raman spectra for all abiogenic $CaCO_3$ had a major peak at $\sim$1088 cm^{-1}, due to the symmetric stretching mode (ν_1) of the carbonate ion (White 2009). Additionally, spectra for abiogenic aragonite samples showed minor peaks at $\sim$208 and $\sim$702 cm^{-1}, while spectra for abiogenic calcite samples showed minor peaks at $\sim$281 and $\sim$712 cm^{-1} (Fig. 2(a) and (b)). The peaks in the 200 cm^{-1} range are attributed to lattice modes, and those in the 700 cm^{-1} range were attributed to the in-plane bending mode (ν_4) of the carbonate ion (Bischoff *et al.* 1985; Urmos *et al.* 1991; Stopar *et al.* 2005; White 2009).

Raman spectra collected with the 785 nm laser exhibited a peak between 1075 and 1092 cm^{-1} for both biogenic and abiogenic $CaCO_3$ (Table 3, Fig. 2(c) and (d)). These results indicated that there is reduced sample fluorescence when using a longer excitation wavelength in Raman measurements, which is ideal in the characterization of minerals containing organic matter; however, additional fluorescence suppression is still needed to obtain peaks for any organic compounds present. The selection of an optimal laser excitation wavelength is an important factor in Raman spectroscopy since different compounds have different sensitivities to a given laser wavelength, and wavelength can affect the level of sample fluorescence emission to the extent in which higher intensity fluorescence peaks can overwhelm the weaker Raman bands (Villar & Edwards 2006). The use of an even longer wavelength (>785 nm) may be successful in reducing sample fluorescence to observe Raman peaks in spectra of these particular biogenic $CaCO_3$ samples.

Laser-induced fluorescence spectroscopy

Abiogenic carbonates did not show any laser-induced fluorescence using the 365 and 405 nm lasers, whereas all biogenic carbonates except *Arthrobacter* sp. (ofe 7.23) exhibited fluorescence (Table 3, Fig. 3(a) and (b)). All biogenic samples except *Arthrobacter* sp. (ofe 7.23, ofe 4.2, ofe 9.29 and cy7) showed fluorescence peaks at $\sim$ 620 and $\sim$682 nm. *Arthrobacter* sp. (ofe 10.10, ofe 8.9, ofe 3.1, ofe 9.29, ofe 1.1, JG9 and ofe 10.25), *Agromyces* sp. (eur3 7.19), and *Rhodococcus* sp. (JG12) showed fluorescence peaks at either $\sim$576, $\sim$578 or $\sim$580 nm. *Agromyces* sp. (eur3 7.19), *Arthrobacter* sp. (ofe 8.9, ofe 3.1, ofe 9.29 and ofe 1.1), *Ralstonia* sp. (ofe 1.3), *Rhodococcus* sp. (cy5 and eur3 9.01.3), *Arthrobacter* sp. (oc825) and *R. mucilaginosa* (JG1) showed fluorescence peaks at either $\sim$498 or $\sim$503 nm. Many samples (ofe 10.25, ofe 10.10, eur3 7.19, ofe 8.9, ofe 3.1, ofe 10.25, ofe 9.29, ofe 1.1, cy7 and JG12) showed fluorescence peaks at $\sim$466. Some samples (ofe 4.2, ofe 10.10, ofe 10.25, cy7 and JG12) also showed peaks at $\sim$520 nm.

Fluorescence peaks observed in the Raman spectra (532 nm) are listed in Table 3 Raman spectra for abiogenic aragonite carbonate samples (CRB120 and CRB125) showed fluorescence peaks at $\sim$596 nm (2018 cm^{-1}) and $\sim$594 nm (1962 cm^{-1}), respectively, while abiogenic calcite (CRB131) showed a peak at $\sim$611 nm (2430 cm^{-1}) (Fig. 2(a) and (b)). Raman spectra for all biogenic carbonates except ofe 9.29 showed fluorescence peaks at either $\sim$582, $\sim$585 or $\sim$596 nm. Raman spectra for many of the biogenic carbonates (isolates ofe 9.29, ofe 7.23, eur3 7.19, ofe 8.9, ofe 3.1, ofe 10.25, ofe 1.1, cy7, oc825, JG9 and JG12) had a fluorescence peak at either $\sim$618, $\sim$620, $\sim$622 or $\sim$630 nm.

Fluorescence may be attributed to the presence of trapped electrons, organic compounds, or trace amounts of transition metals in $CaCO_3$s (Bischoff *et al.* 1985; Urmos *et al.* 1991; Wang & Mullins 1997; Bozlee *et al.* 2005). Organic compounds that emit fluorescence are generally aromatic or conjugated, such as the enzyme cofactors FAD and NADPH, which have emission maxima at $\sim$535 and 440/460 nm, respectively (Ammor 2007). In characterizing biogenic and abiogenic magnesian carbonates with Raman spectroscopy, Bischoff *et al.* (1985) also noted fluorescence in spectra for biogenic samples that at times overwhelmed Raman peaks, and was attributed to the incorporation of trace metal ions, since they are found in virtually all biogenic materials (Bischoff *et al.* 1983, 1985; Veizer 1983). This explanation could account for the lack of fluorescence emission peaks in spectra for our abiogenic samples since they should be of higher purity than the biogenic samples. Raman spectra for biogenic samples often show a weak peak at $\sim$1014 cm^{-1} due to the bicarbonate ion (HCO_3^-), which may be present in order to balance Na^+ charges in biological matrices (White 1975; Bischoff *et al.* 1983, 1985; Veizer 1983).

Implications for astrobiology

Our results indicate that reflectance spectroscopy would be able to discriminate biogenic from abiogenic $CaCO_3$ by numerous absorption features in the visible light region in spectra of biogenic carbonates. However, there are two important caveats: (1) the spectroscopic features that seem to enable discrimination of biogenic from abiogenic carbonates are all associated with the co-existing organic matter in the biogenic samples; and (2) this presumes that the carbonates under investigation are pure and no spectral interferences would be present from any phases that are not of interest for discriminating biogenic from abiogenic carbonates. Also, laser-induced fluorescence spectroscopy could be a useful tool for

https://doi.org/10.1017/S1473550414000366 Published online by Cambridge University Press

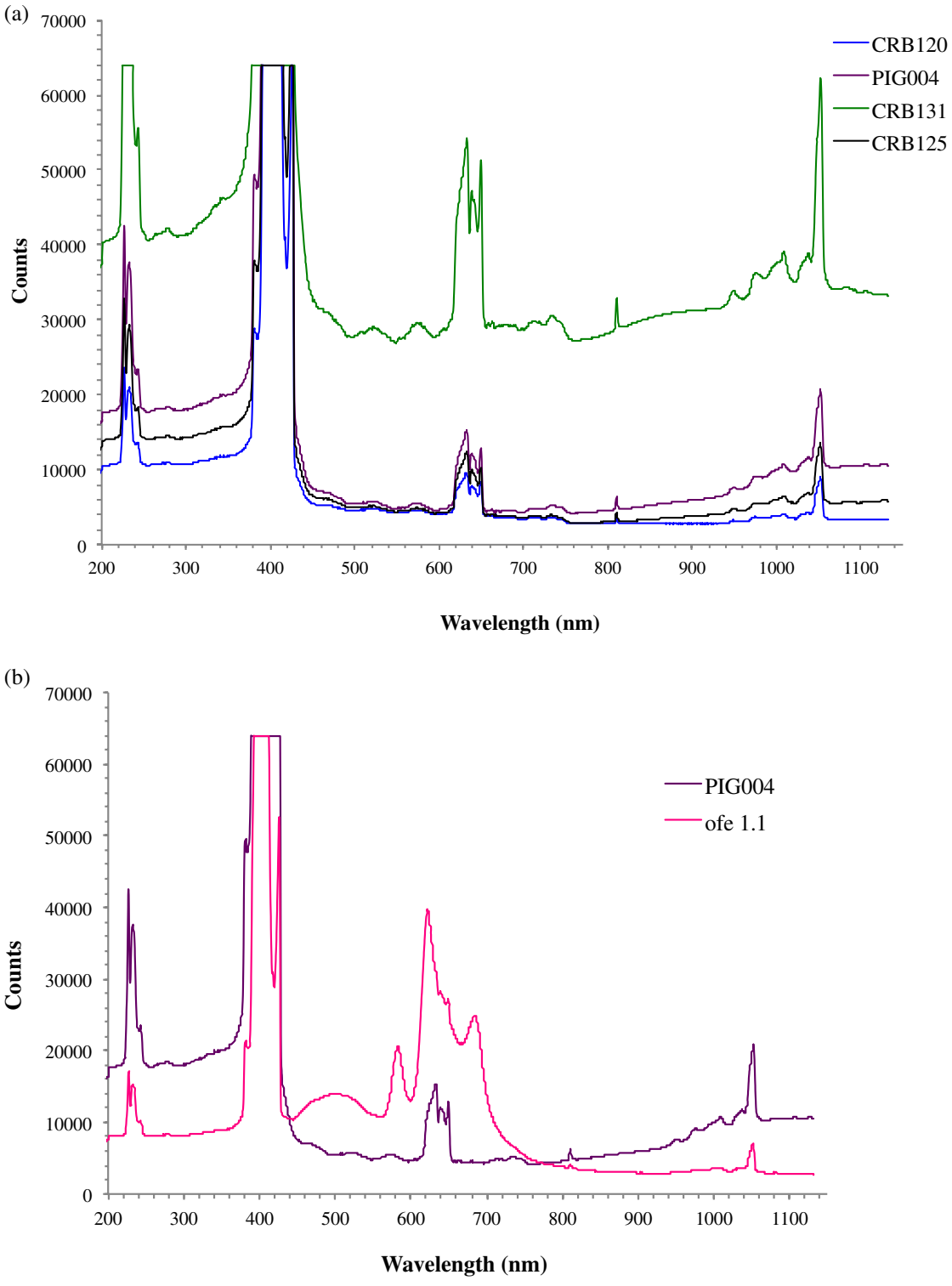

Fig. 3. (a) Laser-induced fluorescence spectra (200–1150 nm) of abiogenic aragonite (CRB120 and CRB125) and calcite (PIG004 and CRB131) collected with a 405 nm light source. (b) Laser-induced fluorescence spectra (200–1150 nm) of abiogenic calcite (PIG004) and biogenic $CaCO_3$ (represented by sample ofe 1.1) collected with a 405 nm light source. The prominent peak near 405 nm and weaker peak near 810 nm are attributable to the laser.

detecting biomarkers, since many fluorescence emission peaks occurred in the visible region upon excitation with 365 and 405 nm light sources; however, it depends on what is causing these peaks. If the fluorescence peaks are in fact due to incorporation of trace elements, then it would be difficult to attribute to biogenicity based on fluorescence spectroscopy alone. Therefore, further analyses would be required in order to confirm the specific organic compounds present.

https://doi.org/10.1017/S1473550414000366 Published online by Cambridge University Press

According to our findings, Raman spectroscopy with a 532 or 785 nm laser may result in sample fluorescence, and overpowering of any Raman peaks for organic material. This could be used as an indicator of the presence of organic molecules which would be consistent with, but not necessarily indicative of, biogenically precipitated carbonates.

One concern in differentiating between biogenic and abiogenic minerals is that a compound having biomimetic properties could lead to the misinterpretation of a mineral as having biological origin. Biomimetic carbonates have been found to be indistinguishable from their biogenic counterparts when analysed by differential thermal analysis, since both exhibit a highly strained crystal structure and similar thermal resistance difference from abiogenic carbonate (Thompson *et al.* 2014). The increased strain causing a lower phase transformation temperature, seen in both biomimetic and biogenic carbonates, may be due to incorporation of organic molecules (e.g. amino acids) (Thompson *et al.* 2014). Therefore, it has been suggested that results from differential thermal analysis of carbonates may not necessarily indicate the presence of life; it may only provide evidence for pre-biotic organics that could have been previously used to form life (Thompson *et al.* 2014). This concern may be extended to spectroscopic discrimination of carbonates, and studies concerning the spectral features of biomimetic carbonates should be carried out in order to detect any similarities between biomimetic and biogenic carbonates.

Biomarkers are variable in stability; therefore the degradation of compounds and their derivatives should be taken into account in the search for extant or extinct life on Mars. On Mars, fossilization and preservation of organic material is enhanced by cold temperatures, and anaerobic, hypersaline and arid conditions (Ellery *et al.* 2002). Over geological time, carotenoids are degraded to isoprenoids via modification of the carotenoid polyene chain by various reactions, with hydrogenation being the most common degradation pathway (Ellery *et al.* 2002; Marshall & Marshall 2010). Haem redox centres of aerobic metabolism are degraded to porphyrins (Suo *et al.* 2007). Isoprenoids and porphyrins are considered to be important as biomarkers since they have been found to remain in the fossil record for extended periods of time and are indicative of biogenicity (Ellery *et al.* 2002).

Future studies

The degradation of biomarkers should be considered when distinguishing biogenic from abiogenic carbonates, since any remnant of life or biological activity on Mars would be subject to degradation over geological time. We are currently conducting further studies investigating the effects of Martian conditions on the spectral and morphological features of biogenic and abiogenic carbonates. These studies will be useful in identifying if and how harsh conditions can modify mineralogical biomarkers in order to better understand the limits of investigative techniques in the discrimination of biogenic from abiogenic minerals.

References

Ammor, M.S. (2007). Recent advances in the use of intrinsic fluorescence for bacterial identification and characterization. *J. Fluoresc*. **17**, 455–459.

Armstrong, G.A. & Hearst, J.E. (1996). Carotenoids 2: genetics and molecular biology of carotenoid pigment biosynthesis. *FASEB J* **10**, 228–237.

Banfield, J.F., Moreau, J.W., Chan, C.S., Welch, S.A. & Little, B. (2001). Mineralogical biosignatures and the search for life on Mars. *Astrobiology* **1**, 447–465.

Barton, L.L. (2005). *Structural and Functional Relationships in Prokaryotes*. Springer, New York.

Bibring, J.-P., *et al.* (2005). Mars surface diversity as revealed by the OMEGA/Mars Express observations. *Science* **307**, 1576–1581.

Bischoff, W.D., Bishop, F.C. & Mackenzie, F.T. (1983). Biogenically produced magnesian calcite; inhomogeneities in chemical and physical properties; comparison with synthetic phases. *Am. Mineral*. **68**, 1183–1188.

Bischoff, W.D., Sharma, S.K. & Mackenzie, F.T. (1985). Carbonate ion disorder in synthetic and biogenic magnesian calcites; a Raman spectral study. *Am. Mineral*. **70**, 581–589.

Blanco, A., Orofino, V., D'Elia, M., Fonti, S., Mastandrea, A., Guido, A. & Russo, F. (2013). Infrared spectroscopy of microbially induced carbonates and past life on Mars. *Icarus* **226**, 119–126.

Boquet, E., Boronat, A. & Ramos-Cormenzana, A. (1973). Production of calcite (calcium carbonate) crystals by soil bacteria is a general phenomenon. *Nature* **246**, 527–529.

Boynton, W.V., Ming, D.W., Kounaves, S.P., Young, S.M.M., Arvidson, R. E., Hecht, M. H., Hoffman, J., Niles, P.B., Hamara, D.K., Quinn, R.C., *et al.* (2009). Evidence for calcium carbonate at the Mars Phoenix landing site. *Science* **325**, 61–64.

Bozlee, B.J., Misra, A.K., Sharma, S.K. & Ingram, M. (2005). Remote Raman and fluorescence studies of mineral samples. *Spectrochim. Acta A, Mol. Biomol. Spectrosc*. **61**, 2342–2348.

Clark, R.N., King, T.V., Klejwa, M., Swayze, G.A. & Vergo, N. (1990). High spectral resolution reflectance spectroscopy of minerals. *J. Geophys. Res. Solid Earth (1978–2012)* **95**, 12653–12680.

Cockell, C.S., Catling, D.C., Davis, W.L., Snook, K., Kepner, R.L., Lee, P. & McKay, C.P. (2000). The ultraviolet environment of Mars: biological implications past, present, and future. *Icarus* **146**, 343–359.

Davis, W.L. & McKay, C.P. (1996). Origins of life: a comparison of theories and application to Mars. *Orig. Life Evol. Biosph*. **26**, 61–73.

De Angelis, S., De Sanctis, M.C., Ammannito, E., Altieri, F., Carli, C., Frigeri, A., Boccaccini, A. & Giardino, M. (2014). Analysis of rocks particulates by VNIR spectroscopy with MA_Miss instrument breadboard. *Lunar and Planetary Science Conference, 45, abstract* #1713.

Delaye, L. & Lazcano, A. (2005). Prebiological evolution and the physics of the origin of life. *Phys. Life Rev*. **2**, 47–64.

Dieser, M., Greenwood, M. & Foreman, C.M. (2010). Carotenoid pigmentation in Antarctic heterotrophic bacteria as a strategy to withstand environmental stresses. *Arct. Antarct. Alpine Res*. **42**, 396–405.

Dworkin, M. & Falkow, S. (2006). *The Prokaryotes: Vol. 7: Proteobacteria: Delta and Epsilon Subclasses. Deeply Rooting Bacteria*. Springer, New York.

Edwards, H.G.M. (2010). Raman spectroscopic approach to analytical astrobiology: the detection of key geological and biomolecular markers in the search for life. *Philos. Trans. Royal Soc. A* **368**, 3059–3065.

Ehlmann, B.L., Mustard, J.F., Murchie, S.L., Poulet, F., Bishop, J.L., Brown, A.J., Calvin, W.M., Clark, R.N., Des Marais, D.J., Milliken, R.E., *et al.* (2008). Orbital identification of carbonate-bearing rocks on Mars. *Science* **322**, 1828–1832.

Ehrlich, H.L. (2002). *Geomicrobiology*, 4th edn. Marcel Dekker, New York.

Ellery, A., Kolb, C., Lammer, H., Parnell, J., Edwards, H., Richter, L., Patel, M., Romstedt, J., Dickensheets, D., Steele, A. & Cockell, C. (2002). Astrobiological instrumentation for Mars – the only way is down. *Int. J. Astrobiol*. **1**, 365–380.

Gaffey, S.J. (1987). Spectral reflectance of carbonate minerals in the visible and near infrared (0.35–2.55 microns): calcite, aragonite, and dolomite. *Am. Mineral*. **71**, 151–162.

https://doi.org/10.1017/S1473550414000366 Published online by Cambridge University Press

Holm, N.G. & Andersson, E. (2005). Hydrothermal simulation experiments as a tool for studies of the origin of life on earth and other terrestrial planets: a review. *Astrobiology* **5**, 444–460.

Izawa, M.R.M., Applin, D.M., Norman, L. & Cloutis, E.A. (2014). Reflectance spectroscopy (350–2500 nm) of solid-state polycyclic aromatic hydrocarbons (PAHs). *Icarus* **237**, 159–181.

Korablev, O., *et al.* (2013). AOTF near-IR spectrometers for study of lunar and martian surface composition. *European Planetary Science Congress 8, abstract* #EPSC2013-50-1.

Mann, S. (2001). *Biomineralization: Principles and Concepts in Bioinorganic Materials Chemistry*. Oxford University Press, New York.

Marshall, C.P. & Marshall, A.O. (2010). The potential of Raman spectroscopy for the analysis of diagenetically transformed carotenoids. *Philos. Trans. Royal Soc. A Math. Phys. Eng. Sci*. **368**, 3137–3144.

Michalski, J.R. & Niles, P.B. (2010). Deep crustal carbonate rocks exposed by meteor impact on Mars. *Nat. Geosci*. **3**, 751–755.

McKay, C.P. (1997). The search for life on Mars. *Orig. Life Evol. Biosp*. **27**, 263–289.

McKay, D.S.D., Gibson, E.K.E., Thomas-Keprta, K.L.K., Vali, H.H., Romanek, C.S.C., Clemett, S.J.S., Chillier, X.D.X., Maechling, C.R.C. & Zare, R.N.R. (1996). Search for past life on Mars: possible relic biogenic activity in martian meteorite ALH84001. *Science* **273**, 924–930.

Moore, M.M., Breedveld, M.W. & Autor, A.P. (1989). The role of carotenoids in preventing oxidative damage in the pigmented yeast, *Rhodotorula mucilaginosa*. *Arch. Biochem. Biophys*. **270**, 419–431.

Morris, R.V., Ruff, S.W., Gellert, R., Ming, D.W., Arvidson, R.E., Clark, B.C., Golden, D.C., Siebach, K., Klingelhöfer, G., Schröder, C., *et al.* (2010). Identification of carbonate-rich outcrops on Mars by the Spirit rover. *Science* **329**, 421–424.

Murchie, S., *et al.* (2007). Compact reconnaissance imaging spectrometer for Mars (CRISM) on Mars Reconnaissance Orbiter (MRO). *J. Geophys. Res.* **112**, E05S03. DOI: 10.1029/2006JE002682.

Nassau, K. (1978). The origins of color in minerals. *Am. Mineral*. **63**, 219–229.

Orofino, V., Blanco, A., D'Elia, M., Licchelli, D. & Fonti, S. (2007). Infrared transmission spectroscopy of carbonate samples of biotic origin relevant to Mars exobiological studies. *Icarus* **187**, 457–463.

Orofino, V., Blanco, A., D'Elia, M., Fonti, S. & Licchelli, D. (2009). Time-dependent degradation of biotic carbonates and the search for past life on Mars. *Planet. Space Sci*. **57**, 632–639.

Pilorget, C., Bibring, J.-P. & the MicrOmega Team (2012). The MicrOmega instrument onboard ExoMars and future missions: an IR hyperspectral microscope to analyze samples at the grain scale and characterize early Mars processes. *Third Conference on Early Mars, abstract* #7006.

Raulin, F. & McKay, C.P. (2002). The search for extraterrestrial life and prebiotic chemistry. *Planet. Space Sci*. **50**, 655.

Ronholm, J., Schumann, D., Sapers, H.M., Izawa, M., Applin, D., Berg, B. L., Vali, H., Cloutis, E.A., Whyte, L.G. (in press). A mineralogical characterization of biogenic calcium carbonates precipitated by heterotrophic bacteria isolated from cryophilic polar regions. *Geobiology*.

Sánchez-Román, M., Romanek, C.S., Fernández-Remolar, D.C., Sánchez-Navas, A., McKenzie, J.A., Pibernat, R.A. & Vasconcelos, C. (2011). Aerobic biomineralization of Mg-rich carbonates: implications for natural environments. *Chem. Geol*. **281**, 143–150.

Schulman, J.H. & Compton, W.D. (1962). *Color Centers in Solids*, vol. 2. Pergamon, Oxford.

Simoneit, B.R.T. (2004). Prebiotic organic synthesis under hydrothermal conditions: an overview. *Adv. Space Res*. **33**, 88–94.

Stalport, F., *et al.* (2005). Search for past life on Mars: physical and chemical characterization of minerals of biotic and abiotic origin: part 1 – Calcite. *Geophys. Res. Lett*. **32**, L23205.

Stalport, F., Person, A., Cabane, M., Ausset, P., Coll, P., Szopa, C. & Navarro-Gonzalez, R. (2008). Biominerals on Mars: the potential for carbonates to be life indicators. In *37th COSPAR Scientific Assembly*, 37, p. 3017.

Steven, B., Briggs, G., McKay, C.P., Pollard, W.H., Greer, C.W. & Whyte, L.G. (2007). Characterization of the microbial diversity in a permafrost sample from the Canadian high Arctic using culture-dependent and culture-independent methods. *FEMS Microbiol. Ecol*. **59**, 513–523.

Stopar, J.D., Lucey, P.G., Sharma, S.K., Misra, A.K., Taylor, G.J. & Hubble, H.W. (2005). Raman efficiencies of natural rocks and minerals: performance of a remote Raman system for planetary exploration at a distance of 10 meters. *Spectrochim. Acta A, Mol. Biomol. Spectrosc*. **61**, 2315–2323.

Storrie-Lombardi, M.C. & Sattler, B. (2009). Laser-induced fluorescence emission (L.I.F.E.): in situ nondestructive detection of microbial life in the ice covers of Antarctic lakes. *Astrobiology* **9**, 659–672.

Suo, Z., Avci, R., Schweitzer, M.H. & Deliorman, M. (2007). Porphyrin as an ideal biomarker in the search for extraterrestrial life. *Astrobiology* **7**, 605–615.

Thompson, S.P., Parker, J.E. & Tang, C.C. (2014). Thermal breakdown of calcium carbonate and constraints on its use as a biomarker. *Icarus* **229**, 1–10.

Thöny-Meyer, L. (1997). Biogenesis of respiratory cytochromes in bacteria. *Microbiol. Mol. Biol. Rev*. **61**, 337–376.

Tucker, E.M. & Wright, V.P. (1990). *Carbonate Sedimentology*. Blackwell Scientific Publications, Oxford, pp. 482.

Urmos, J., Sharma, S.K. & Mackenzie, F.T. (1991). Characterization of some biogenic carbonates with Raman spectroscopy. *Am. Mineral*. **76**, 641–646.

Vecht, A. & Ireland, T.G. (2000). The role of vaterite and aragonite in the formation of pseudo-biogenic carbonate structures: implications for Martian exobiology. *Geochim. Cosmochim. Acta* **64**, 2719–2725.

Veizer, J. (1983). Trace elements and isotopes in sedimentary carbonates. *Rev. Mineral. Geochem*. **11**, 265–299.

Villar, S.E.J. & Edwards, H.G. (2006). Raman spectroscopy in astrobiology. *Anal. Bioanal. Chem*. **384**, 100–113.

Wang, J. & Mullins, O.C. (1997). Fluorescence of limestones and limestone components. *Appl. Spectrosc*. **51**, 1890–1895.

White, A.F. (1975). Sodium and potassium coprecipitation in calcium carbonate. *PhD Thesis*, Northwestern University.

White, S.N. (2009). Laser Raman spectroscopy as a technique for identification of seafloor hydrothermal and cold seep minerals. *Chem. Geol*. **259**, 240–252.

Workman, J. Jr. & Weyer, L. (2012). *Practical Guide and Spectral Atlas for Interpretive Near-Infrared Spectroscopy*. CRC Press, Boca Raton.

https://doi.org/10.1017/S1473550414000366 Published online by Cambridge University Press